Received 23 November 2023; revised 28 January 2024; accepted 5 February 2024. Date of publication 13 February 2024; date of current version 26 March 2024.

Digital Object Identifier 10.1109/OJAP.2024.3365539

A Novel Yagi Element Integrated Nested Loop Quasi-Self-Complementary Dual-Port Combiner Radiator

R. GOPIKA [1] (Graduate Student Member, IEEE), CHINMOY SAHA [1] (Senior Member, IEEE), AND YAHIA M. M. ANTAR [2] (Life Fellow, IEEE)

[1] 1Department of Avionics, Indian Institute of Space Science and Technology, Thiruvananthapuram 695547, India

[2] Department of Electrical and Computer Engineering, Royal Military College, Kingston, ON K7K 7B4, Canada

CORRESPONDING AUTHOR: R. GOPIKA (e-mail: gopikar@ieee.org)

This work was supported in part by the Science and Engineering Research Board, Department of Science and Technology, Government of India, under the DST Core Grant Scheme under Grant CRG/2019/004570.

ABSTRACT This article presents a quasi-self-complementary radiator structure designed to operate simultaneously as a combiner and an antenna. The dual-port architecture comprises axially symmetric nested microstrip loops. The upper half of the radiator structure placed on the top plane is nearly complementary to the lower half on the bottom plane. The nested loop is loaded with a Yagi element for improved performance. This additional element in the radiator enhances the end-fire radiation from the nested loop wideband dual port structure without disturbing the parallel combiner action. An additional gain of nearly 3 dB is obtained with this element across the operating bandwidth. Measurement of both the fabricated prototypes, with and without the Yagi element, reveal the desired parallel combiner action for an operating range of 1.8-2.3 GHz with good matching. The quasi-self-complementary nested loop architecture offers a wide operational bandwidth. The proposed radiator structure is a compact and low-loss alternative for antenna arrays.

INDEX TERMS Combiner, dual-port, radiator, self-complementary.

I. INTRODUCTION

MICROWAVE power combiners/dividers are integral components for the practical realization of any wireless system. Design of these passive networks, when associated with antenna arrays, become increasingly crucial in both transmitter and receiver systems as the network losses can degrade the system efficiency. The transmission-line implementation of passive microwave power combiner/divider networks significantly affects the system performance based on various factors like choice of transmission line, line length, transmission line junction, etc. The parasitic effects and associated losses inherent in a practically realized microwave junction may be significantly mitigated when the antenna is modified to perform the combiner/divider function additionally.

Thus, the cascaded network of the power combiner/divider and the single-port antenna must be replaced to improve system performance. The resultant new structure, named as multi-port radiator, should perform, both as an antenna and a combiner/divider, and hence, can be connected directly to the preceding system. A generic schematic of a transceiver system indicating basic power combiner/divider replacing with a two-port radiator is shown in Fig. 1. Naturally, this improves the overall system compactness, as the functionality remains unaffected. Such antenna architectures which incorporate multiple feeds to facilitate specific functionalities besides the radiation are generally termed Multi-Port Driven (MPD) structures [1]. The desired current distribution is achieved with numerous ports, leading to potential features like power combining/dividing and impedance matching. Unlike a conventional antenna, an MPD structure offers additional features besides radiation and is often referred to as a 'radiator' [1].

Since the additional functionality considered in this paper, power combining/dividing, is reciprocal, the term combiner is used instead of combiner/divider for the rest of the article.

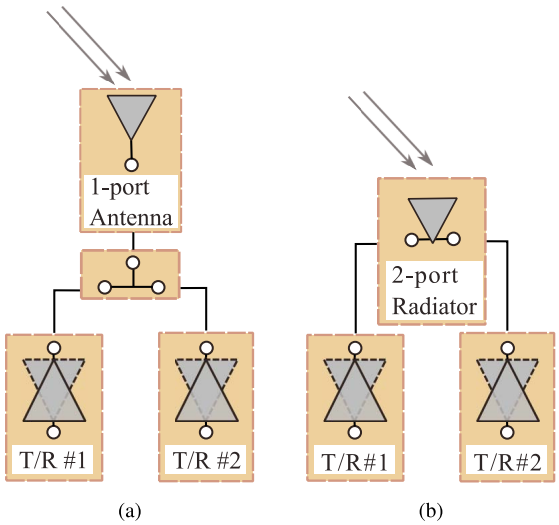

FIGURE 1. Schematic representation of transceiver system (T/R refers the transmit/receive systems): (a) Single port antenna fed with a power combiner/divider network connecting the preceding transceiver modules. (b) Dual-port radiator replacing the conventional power combiner/divider network without affecting the radiation and passive network characteristics.

Implementation of on-antenna power combination architectures implemented with cavities [2], [3], [4], patches [5], [6], [7], slots [8], [9], [10] and loops [11], [12], [13], [14], [15], [16] have been previously reported. However, these single-frequency resonant structures fail to provide a reasonable bandwidth for the combiner action. Conventional combiner radiator architectures yield a relatively narrow bandwidth, demanding strict fabrication tolerances to obtain satisfactory performance. Thus, achieving a wider combiner bandwidth is a critical demand for the design of combiner cum radiator for microwave applications.

This article proposes a new combiner radiator with a nested loop structure arranged in quasi-self-complementary geometry. The proposed architecture offers novel features of wider usable bandwidth and end-fire radiation. The enhanced usable bandwidth includes combiner and radiator nature besides the good impedance matching of the proposed structure. Thus, in contrast to the single loop resonant radiators, which enable combiner action only at a single frequency point, the proposed structure ensures easier integration with other subsystems. Furthermore, the end-fire radiation of the structure facilitates the possibility of in-plane Yagi element insertion which acts like a director and enhances the radiator gain without impairing the combiner action. The detailed performance of the proposed radiator is systematically measured and presented. Radiator geometry, the combiner function and end-fire radiation are discussed in Section II. Section III deals with the results and discussions of the proposed radiator.

II. RADIATOR DESIGN

A. RADIATOR GEOMETRY

The proposed quasi-self-complementary (QSC) radiator with integrated in-plane Yagi element is shown in Fig. 2. As indicated, the nested loop structure on the top plane is

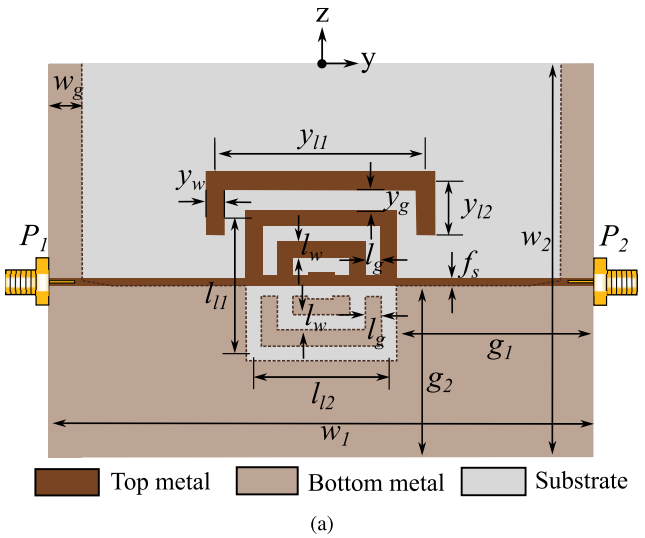

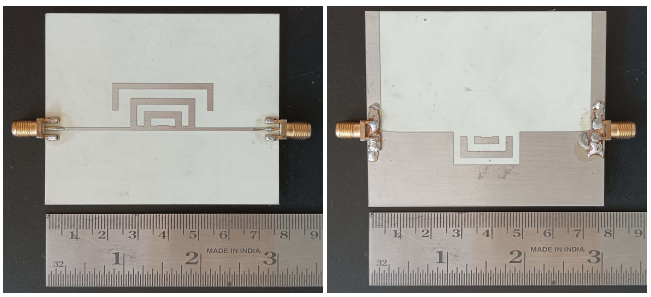

FIGURE 2. (a) Geometry of the proposed quasi-self-complementary dual-port radiator. (b) Top and (c) bottom view of fabricated prototype.

axially complementary to the bottom plane structure. The radiator structure has outer and inner loops with a mean perimeter equal to the integer multiple of the highest and lowest wavelength of combiner bandwidth as governed by (1) and (2).

$$2(l_{l1} + l_{l2}) = n\lambda_h, n = 1, 2, \ldots, \quad (1)$$

$$2\left(l_{l1} + l_{l2} - 4l_w - 4l_g\right) = m\lambda_l, m = 1, 2, \ldots, \quad (2)$$

where, λ_h and λ_l are the highest and lowest wavelengths of the combiner bandwidth. The loop widths on the top metal plane, 'l_w', are the same as the slot widths of the bottom plane and thus comply with the desired self-complementary design. A similar relation holds for the slot widths of the top plane, 'l_g', and the loop widths of the bottom plane. A Yagi element of length (y_{l1}+2y_{l2}) and width 'y_w' is placed at a distance 'y_g' away from the edge of the nested loop on the top plane to ensure improved end-fire radiation.

The 50 Ω microstrip line feeds, P_1 and P_2, are placed on the diametrically opposite edges of the top plane of the nested loop radiator. Since the structure is not entirely complementary along the horizontal axis (due to the presence of the partial ground plane), the proposed dual-port radiator is structurally 'quasi-self complementary'.

The proposed QSC radiator is designed on a low-loss RF laminate Rogers RO4350B ($\epsilon_r = 3.66$, tan $\delta = 0.002$)

TABLE 1. Proposed radiator dimensions (mm).

h=0.762 mm, ϵ_r= 3.66, tan δ = 0.002						
l_{l1}	l_{l2}	y_{l1}	y_{l2}	y_w	l_w	l_g
20	20	32	7.5	2	2.2	2.2
w_1	w_2	g_1	g_2	m_1	m_2	w_g
76	62	27.4	24	4.26	0.4	4.5
Overall size ($w_1 \times w_2 \times h$)				76×62×0.762		

of thickness 30 mils. All the dimensions of the radiator are listed in Table 1. The overall size of the radiator is 76×62 mm^2. Images of the fabricated prototype with integrated Yagi element are shown in Fig. 2(b) and Fig. 2(c).

B. WIDEBAND COMBINER

The combiner networks, based on the feeding port features, in general, may be classified into two: series and parallel. The former ensures equal port currents, whereas the latter assures equal input port voltages. Thus, the characteristic matrices of the series and parallel combiners are admittance and impedance matrices, respectively. For a two-port combiner network, all four elements of the characteristic matrix remain equal. As the proposed structure is a parallel combiner due to the unbalanced feed nature, the impedance matrix is,

$$[Z] = \begin{bmatrix} Z_i & Z_i \\ Z_i & Z_i \end{bmatrix}$$

where, 'Z_i' is the single port antenna input impedance.

In [13], [14], [15], [16], single loop architectures with a circumference of an integer multiple of operating wavelength, as mentioned in the previous section, are conceived to achieve the desired characteristic impedance matrix of the combiner radiators. The ports are placed on the loop with a distance of half wavelength in between. Symmetrical port placements are usually preferred to ensure that both Z_{11} and Z_{22} are equal. With such an architecture, for a two-port parallel combiner loop, Z_{21} will be equal to Z_{11}, as the open circuit voltage at port-2 is the same as that of port-1. However, these structures offer combiner action only for a single frequency point, as both the magnitude and phase of the port-2 voltage differ from the port-1 voltage due to the wavelength dependency. Hence, such configurations impose a practical challenge in incorporating the combiner radiator with wideband circuits.

Here, the nested loop architecture presents multiple current paths of varying lengths, as indicated in (1)-(2), which correspond to the required operational wavelength range. When the feeds are placed equidistant from the centre of the axially symmetrical structure with an integer multiple of the operating wavelength as the distance of separation, the electric fields at the feeds become identical. Hence, for an impedance matrix calculation, the open circuit condition implies identical values for port-1 and -2 excitations, leading to equal Z_{11} and Z_{21} values. Thus, with both 'n' and 'm' values opted as unity in equations (1) and (2), the proposed structure works as an excellent combiner as well as radiator. This approach ensures equal voltage levels at the ports for the open circuit conditions and thereby offers an improved operating bandwidth. Additionally, the axial self-complementary architecture is opted to achieve the constant impedance property [17], [18]. However, due to the practical realization of the balun and inherent extensions in the ground plane, the structure is 'quasi-self-complementary'.

The nested loop in the proposed QSCR is to be excited with a balanced feed. As the SMA connector and the microstrip lines used for the practical feed are unbalanced, a balun is essential for the radiator operation. The ground strips of dimensions ($W_2 \times W_g$) are housed to ensure balun performance, ground connection to the connector and mechanical stability during the pattern measurement at the feeding points. In addition to the balun performance these strips ensure better input matching. However, as the structure is multi-port, isolation between the ports is equally crucial. With good input matching and isolation, the radiator performance may be improved.

C. END-FIRE RADIATION

The combiner radiators explored so far in the literature are broadside in nature. The microstrip [5], [6], [7], [11], [12], [13], [14], [15], [16] and slot [8], [9], [10] radiators discussed previously in the literature facilitate the radiation normal to the antenna plane. However, several applications, such as wireless communication [19], [20], on-body [21], [22] and vehicular applications [23] demand compact endfire radiators. The proposed structure radiates in the end-fire direction with improved gain by keeping the form factor unchanged. The antipodal arrangement of the axially complementary nested loop structure with the extended ground plane of width 'w_g' ensures a focused beam.

A Yagi architecture usually consists of a driven element, a reflector and a director. In the proposed structure, the nested loop acts as the driven element. Feeding ports, P_1 and P_2 excite the loop and initiate the radiation. However, the antipodal ground, the axially symmetric half of the quasi-self-complementary design, acts as a reflector and realizes end-fire radiation in the structure. This radiation towards the Z-direction is enhanced further with a director element, the microstrip line of length $y_{11}+2y_{12}$. The director improves the gain of the nested loop radiator, keeping the form factor of the antenna unchanged. This element is nearly half the wavelength of the centre frequency to achieve the gain improvement in the desired frequency range. This director is placed at a distance of 'y_g' from the outer loop to orient the end-fire radiation from the QSC radiator in the Z direction.

III. RESULTS AND DISCUSSIONS

The proposed dual-port QSC radiator is numerically analysed using a finite element method (FEM) based 3D EM solver [24] and validated with measurements from Agilent PNA N5224A network analyser.

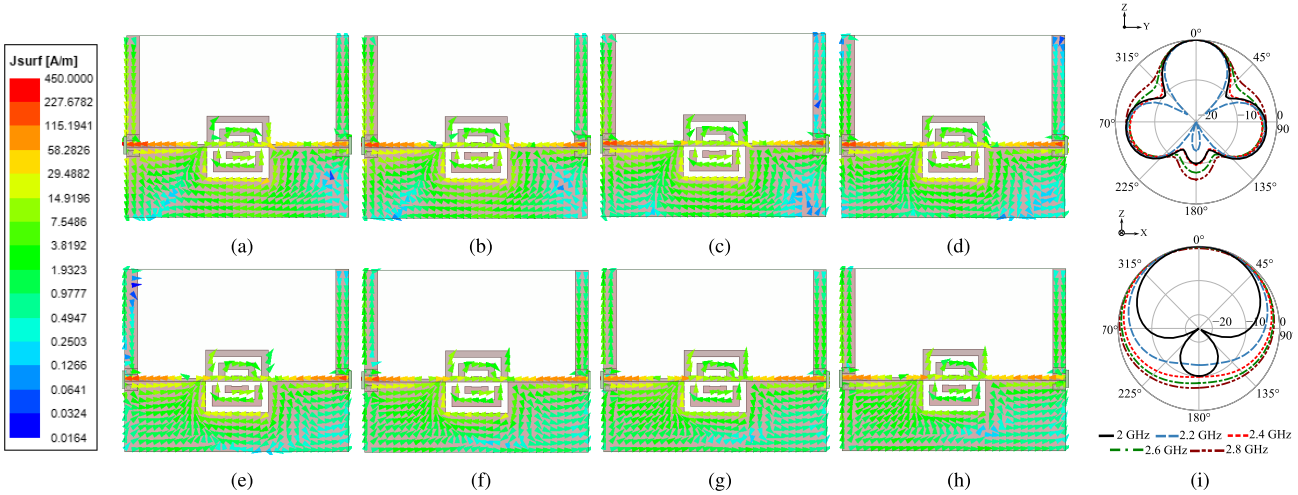

FIGURE 3. Vector plot of surface current density on the proposed dual-port quasi-self-complementary radiator at various frequencies: (a) 2.1 GHz, (b) 2.2 GHz, (c) 2.3 GHz, (d) 2.4 GHz, (e) 2.5 GHz, (f) 2.6 GHz, (g) 2.7 GHz, (h) 2.8 GHz (i) Normalized radiation patterns of the QSCR without Yagi for various frequencies.

Fig. 3 shows the vector plot of the surface current density (J_{surf}) obtained from the 3D EM solver [24] for a frequency range of 2.1-2.8 GHz with a step size of 0.1 GHz. For an operating frequency range of 2.2-2.7 GHz when a single port is excited, surface current density follows nearly the same direction and magnitude at the input ports. This correlation indicates and ensures an equal value for all the elements in the impedance matrix, leading to the parallel combiner performance in this frequency range. For other frequencies, as shown in Fig. 3(a) and Fig. 3(h), the current densities at the ports are observed to differ either in magnitude or in direction.

Fig. 3(i) depicts the normalized radiation patterns for various frequencies. The surface currents in all the frequencies shown in Fig. 3 of the manuscript have an aligned direction through the horizontal strip connecting the feeding ports. The current magnitude is enhanced or diminished based on the current direction in the loop paths. For frequencies below 2.4 GHz, the currents in the nested loop of the upper half have the same effective direction in all loops, causing a directional beam. But for frequencies above 2.4 GHz, the resultant current direction is attributed mainly to the horizontal strip, leading to a less directional beam. The currents in the ground plane also have a vital role in the radiation modes in the QSCR as the ground acts as a reflector to the radiation from the currents in the nested loop upper half. Thus, the patterns alter with frequencies.

Fig. 4 exhibits the simulated and measured impedance matrix parameters of the radiator with and without the Yagi element. Due to the structural symmetry and identical port conditions, only the magnitude and phase of Z_{11} and Z_{21} are shown (Due to the symmetry of the structure, Z_{11}=Z_{22} and reciprocity enforces, Z_{12}=Z_{21}). As mentioned in (3), the combiner feature for the structure is ensured if Z_{11} and Z_{21} are equal for the operating range. The proposed radiator, as revealed from Fig. 4(c) and 4(d), exhibits identical combiner action around 2.4 GHz and 2 GHz, respectively. The shaded portion in the plots of Fig. 4 indicates the frequency range over which the measured Z_{11} and Z_{21} (both magnitude and phase) presents almost identical values with deviation less than 5%. The shift in frequency and magnitude of the simulated and measured impedance results are due to the connectors and adaptors used during the impedance measurement. As revealed in Fig. 4(e) and Fig. 4(f), by incorporating the connector with QSCR, the simulated results follow a closer match with the measured results. Thus, with these additional electrical lengths introduced during the measurement, the results vary from the numerically obtained results. The region of combiner bandwidth with less than 5% deviation between Z_{11} and Z_{21} spans 0.5 GHz (1.8-2.3 GHz) with a fractional bandwidth of 25%. The wider combiner bandwidth of the proposed dual-port radiator with very wideband magnitude and phase matching is due to the nested loop architecture conceived in the design.

The radiation characteristic of the fabricated QSC radiator prototype is measured in a fully calibrated anechoic chamber, with the proposed structure placed on the antenna mount, as shown in Fig. 5(a) and Fig. 5(b). A broadband double ridge horn antenna operating for 0.8-18 GHz is employed as the transmitter, whereas the fabricated QSC radiator is kept in receiving mode. The normalized measured radiation patterns of the proposed radiator for the two orthogonal planes of *XZ* and *YZ*, at 2 GHz, are shown in Fig. 6(c) and Fig. 6(d), and compared with that of the simulated pattern. The two ports of the structure are excited with equal magnitude and opposite phases for a constructive radiation pattern. As revealed from the plots, the measured pattern, i) exhibits good correspondence with that of the simulated pattern in general and ii) closely follows the simulated patterns for a range of $-30°$ to $+30°$ in all the planes. For the self-complementary architecture, excitation should be differential to feed the complementary halves. A balun transition is incorporated for suitable feeding and proper impedance matching. Thus, with the radiating performance of a loop as the fundamental component, the omnidirectional

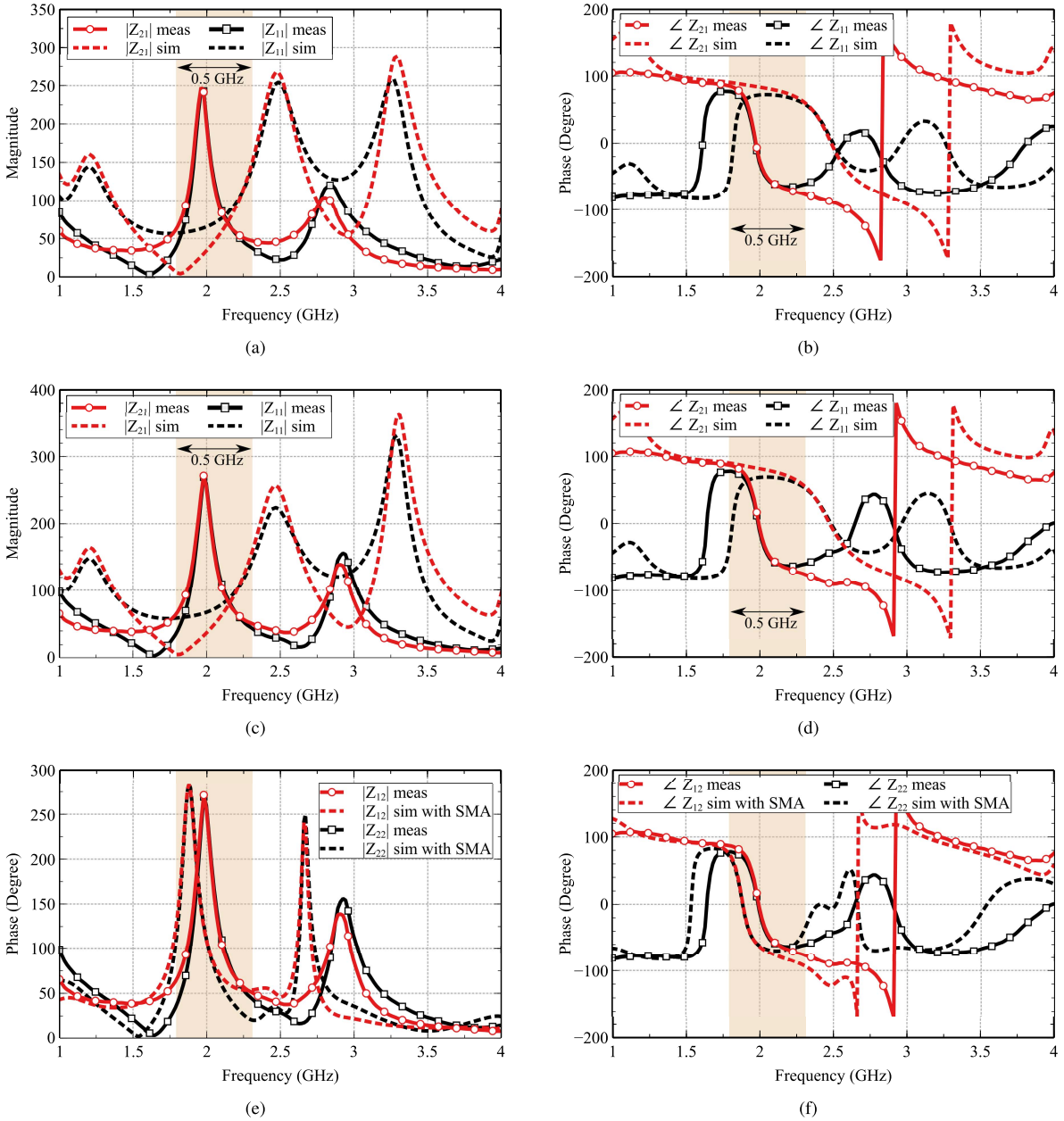

FIGURE 4. Impedance matrix parameters, Z_{11} and Z_{21} of the radiator: (a) Magnitude and (b) Phase for QSC radiator without Yagi element. (c) Magnitude of and (d) phase for QSC radiator with Yagi element.(e) Magnitude of and (f) phase for QSC radiator with Yagi element compared against SMA connector models in the numerical analysis. The dashed and solid lines denote the simulated and measured results respectively.

pattern gets focused on the director and reflector ground. Even though the additional ground strips are a part of the balun action, the effect of these strips causes a more directional YZ plane pattern. However, metal planes are unavailable in the orthogonal XZ plane to ensure an enhanced directional beam, leading to a broader beam. Minor kinks observed near $\pm 45°$ might be due to the reflections from the SMA connectors used at the feed ports P_1 and P_2. Fig. 7(a) shows the S_{ii} magnitude, both simulated and measured, for the radiator. As the plot reveals, the proposed radiator offers good matching over an operating range of 1.5-2.75 GHz.

Fig. 7(b) exhibits the measured gain versus frequency plot of the proposed nested loop self-complementary radiator without and with the Yagi element. The graph reveals that the radiator without the Yagi element yields a peak gain of 0.05-3.98 dBi over 1.5-3 GHz with a maximum of 3.98 dBi at 2.39 GHz. But, the radiator augmented with the Yagi element provides a peak gain of 0.87-5.93 dBi over 1.5-3 GHz with a peak value of 5.93 dBi at 2.54 GHz. Thus, in addition to excellent combiner performance, the proposed Yagi-loaded nested loop self-complementary antenna yields excellent radiation performance.

As the proposed structure is of dual-port architecture, lower values of S_{ii} and S_{ij} are desirable, so that good port matching and isolation are ensured. However, a shift towards lower frequency is observed during the measurement, as

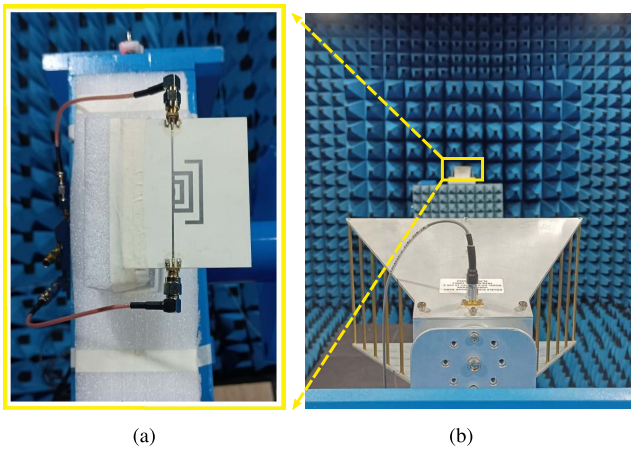

(a) (b)

FIGURE 5. (a) Top view of the radiator mounted for pattern and gain measurement. (b) Radiator along with the reference antenna inside the fully calibrated anechoic chamber.

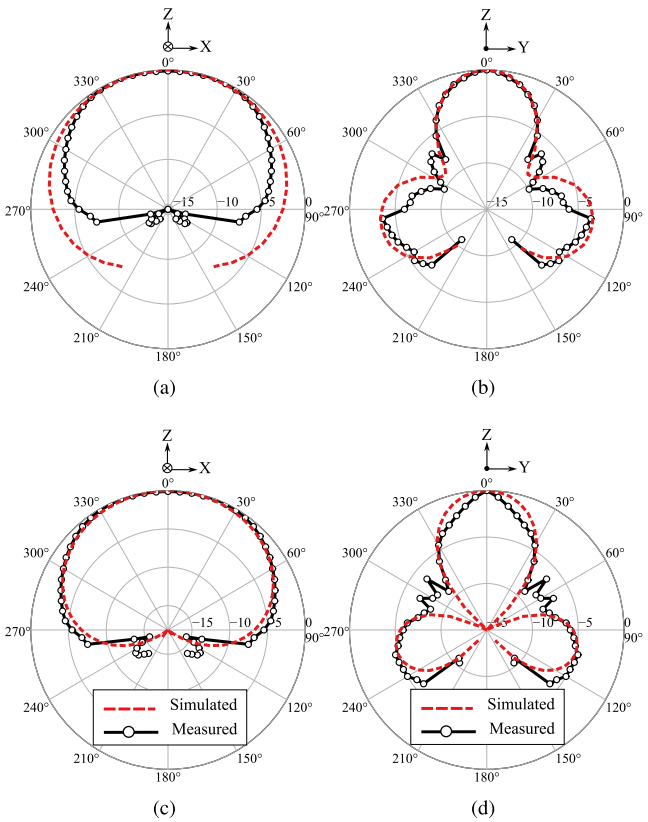

FIGURE 6. Normalized radiation patterns of the radiator at 2 GHz:(a) XZ plane and (b) YZ plane for the QSC radiator without Yagi element. (c) XZ plane and (d) YZ plane for the QSC radiator with Yagi element. The dashed and solid lines denote the simulated and measured results respectively. The measurements are obtained with P_1 and P_2 excited with equal magnitude but opposite phase.

shown in Fig. 4, whereas, the gain enhancement due to the director remains unchanged as that of the numerical analysis. This is due to the proximity feeding of the Yagi element, whose gain performance remains unaffected as the connectors and adapters cannot impact the element directly. Thus, for frequencies with lower S_{ij} and S_{ii}, good realized gain values might occur even when the impedance matching is poor.

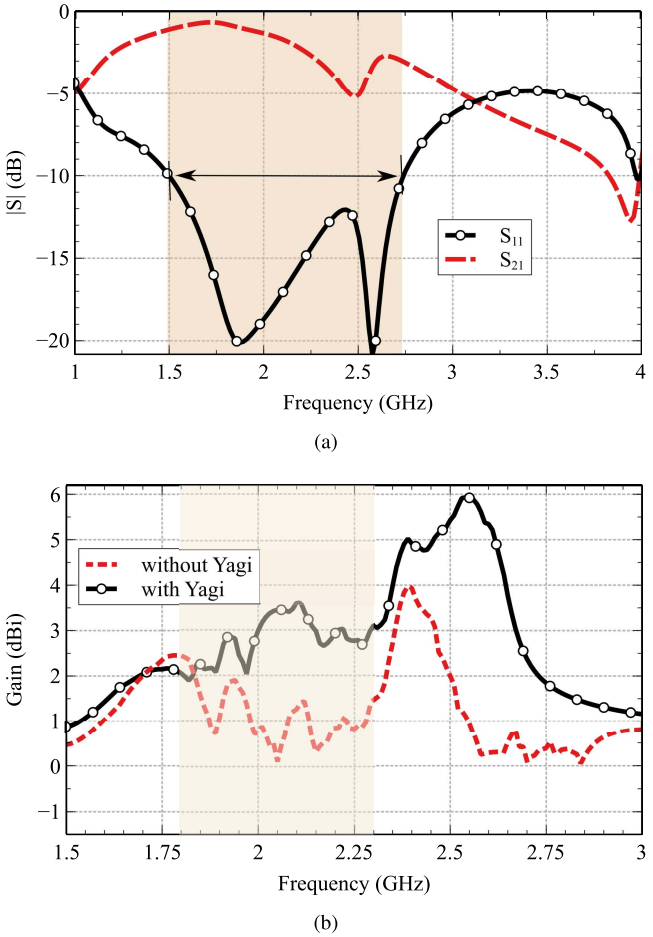

FIGURE 7. (a) Magnitude of S_{ii} Vs frequency. (b) Gain Vs frequency for the radiators.

TABLE 2. Usable bandwidth of the proposed radiator.

Impedance		Combiner		Gain		Usable	
GHz	%	GHz	%	GHz	%	GHz	%
1.2	57	0.5	25	1.5	67	0.5	25

Table 2 portrays the consolidated summary of the proposed QSC radiator. As may be noted, the usable bandwidth of the structure is the intersecting operating range obtained from the impedance bandwidth measured from $|S_{ii}| < -10$ dB, gain above 0 dBi and combiner bandwidth having impedance parameter deviation less than 5%. Table 3 summarizes the comparative analysis of the proposed dual-port radiator architecture performance with previously reported structures. It may be noted that the comparison of compactness remains unbiased and fare when radiators fabricated with similar processes are considered. As some of the works [13], [14] included in Table 3 for the comparison are on-chip radiators, due to the inherent multilayered architecture, process involved and the type of insulator employed, the overall size might be significantly less than the conventional radiators designed on dielectric laminates. However, proposed structure with reasonable size, provides the highest impedance

TABLE 3. Performance comparison with other loop combiner radiators.

Ref	f_0 (GHz)	Bandwidth (%)		Peak Gain (dBi)	Size ($\lambda\times\lambda$)	Remarks
		Combiner BW	Impedance BW			
[11]	38.5, 73.5	-	13, 14	2.9, 3	3.75×7.5	Rogers RO3003 (ϵ_r = 3) substrate
[13]	65	9	-	4.5	0.37×0.41	45 nm CMOS SOI (Silicon on Insulator) process based on-chip radiator
[14]	28	14.3	53.5	3.1	0.12×0.12	45 nm CMOS SOI (Silicon on Insulator) process based on-chip radiator
QSCR	**2**	**25**	**57**	**3.7**	4.13×5	Rogers RO4350B (ϵ_r = 3.66) substrate

and combiner bandwidth with good gain and thereby exhibits great potential for various practical applications.

IV. CONCLUSION

This article proposes a quasi-self-complementary nested-loop radiator designed to work simultaneously as a combiner and an antenna. The dual port structure consists of nested loops with the upper half nearly complementary to the lower half, enabling end-fire radiation and a Yagi element for enhanced gain. The proposed QSC dual-port radiator provides excellent combiner and radiation performance with absolute bandwidths of 500 MHz (1.8-2.3 GHz) and 1.2 GHz (1.5-2.7 GHz), respectively. The main attributes of the radiator, wide bandwidth and high end-fire gain, are attained with quasi-self-complementary geometry and the Yagi element conceived in the design. Thus, the structure can replace the passive combiner networks in an active system where compactness and low-profile nature are the prime requirements.

REFERENCES

[1] S. M. Bowers and A. Hajimiri, "Multi-port driven radiators," *IEEE Trans. Microw. Theory Techn.*, vol. 61, no. 12, pp. 4428–4441, Dec. 2013.

[2] J. G. Marin, A. A. Baba, J. Hesselbarth, R. M. Hashmi, and K. P. Esselle, "Millimeter-wave low-loss multifeed superstrate-based antenna," *IEEE Trans. Antennas Propag.*, vol. 68, no. 5, pp. 3387–3396, May 2020.

[3] P. Nazari, S. Jafarlou, and P. Heydari, "Analysis and design of a millimeter-wave cavity-backed circularly polarized radiator based on fundamental theory of multi-port oscillators," *IEEE J. Solid-State Circuits*, vol. 52, no. 12, pp. 3293–3311, Dec. 2017.

[4] M. W. Mansha and M. M. Hella, "A 148-GHz radiator using a coupled loop oscillator with a quad-feed antenna in 22-nm FD-SOI," *IEEE J. Solid-State Circuits*, vol. 56, no. 5, pp. 1514–1526, May 2021.

[5] S. Gao and P. Gardner, "Integrated antenna/power combiner for LINC radio transmitters," *IEEE Trans. Microw. Theory Techn.*, vol. 53, no. 3, pp. 1083–1088, Mar. 2005.

[6] R. Kormilainen, J.-M. Hannula, T. O. Saarinen, A. Lehtovuori, and V. Viikari, "Realizing optimal current distributions for radiation efficiency in practical antennas," *IEEE Antennas Wireless Propag. Lett.*, vol. 19, pp. 731–735, 2020.

[7] T. Le Gall, A. Ghiotto, S. Varault, G. Morvan, B. Louis, and G. Pillet, "Quadruple-fed aperture-coupled microstrip patch antenna for on-antenna power combining," in *Proc. 51st Eur. Microw. Conf. (EuMC)*, 2022, pp. 55–58.

[8] S. Li, T. Chi, and H. Wang, "Multi-feed antenna and electronics co-design: An E-band antenna-LNA front end with on-antenna noise-canceling and G_m-boosting," *IEEE J. Solid-State Circuits*, vol. 55, no. 12, pp. 3362–3375, Dec. 2020.

[9] B. Goettel, P. Pahl, C. Kutschker, S. Malz, U. R. Pfeiffer, and T. Zwick, "Active multiple feed on-chip antennas with efficient in-antenna power combining operating at 200–320 GHz," *IEEE Trans. Antennas Propag.*, vol. 65, no. 2, pp. 416–423, Feb. 2017.

[10] T. Chi, J. S. Park, S. Li, and H. Wang, "A millimeter-wave polarization-division-duplex transceiver front-end with an on-chip multifeed self interference-canceling antenna and an all-passive reconfigurable canceller," *IEEE J. Solid-State Circuits*, vol. 53, no. 12, pp. 3628–3639, Dec. 2018.

[11] S. Li, T. Chi, Y. Wang, and H. Wang, "A millimeter-wave dual-feed square loop antenna for 5G communications," *IEEE Trans. Antennas Propag.*, vol. 65, no. 12, pp. 6317–6328, Dec. 2017.

[12] M. Kashanianfard and K. Sarabandi, "An accurate circuit model for input impedance and radiation pattern of two-port loop antennas as E- and H-probe," *IEEE Trans. Antennas Propag.*, vol. 65, no. 1, pp. 114–120, Jan. 2017.

[13] H. T. Nguyen, T. Chi, S. Li, and H. Wang, "A linear high-efficiency millimeter-wave CMOS doherty radiator leveraging multi-feed on-antenna active load modulation," *IEEE J. Solid-State Circuits*, vol. 53, no. 12, pp. 3587–3598, Dec. 2018.

[14] S. Li, T. Chi, J.-S. Park, H. T. Nguyen, and H. Wang, "A 28-GHz flip-chip packaged Chireix transmitter with on-antenna outphasing active load modulation," *IEEE J. Solid-State Circuits*, vol. 54, no. 5, pp. 1243–1253, May 2019.

[15] R. Gopika, C. Saha, and Y. M. M. Antar, "Balun-integrated dual port antenna for RF energy harvesting applications," in *Proc. IEEE Indian Conf. Antennas Propag. (InCAP)*, 2021, pp. 736–738.

[16] R. Gopika and C. Saha, "Differential loop rectenna unit for extendable large arrays," in *Proc. Wireless Power Week (WPW)*, 2022, pp. 388–391.

[17] Y. Mushiake, "Constant-impedance antennas," *J. Inst. Electron., Inf. Commun. Eng.*, vol. 48, no. 4, pp. 580–584, Apr. 1965.

[18] Y. Mushiake, *Self-Complementary Antennas: Principle of Self-Complementarity for Constant Impedance*. London, U.K.: Springer, 2012.

[19] J. Wang, F. Wu, D. Jiang, and K.-M. Luk, "A leaky-wave magnetoelectric antenna with endfire radiation for millimeter-wave communications," *IEEE Trans. Antennas Propag.*, vol. 71, no. 4, pp. 3654–3659, Apr. 2023.

[20] Z. Zhang, X. Cao, J. Gao, S. Li, and J. Han, "Broadband SIW cavity-backed slot antenna for endfire applications," *IEEE Antennas Wireless Propag. Lett.*, vol. 17, pp. 1271–1275, 2018.

[21] K. Agarwal, Y.-X. Guo, and B. Salam, "Wearable AMC backed near-endfire antenna for on-body communications on latex substrate," *IEEE Trans. Compon., Pack. Manuf. Technol.*, vol. 6, no. 3, pp. 346–358, Mar. 2016.

[22] N. Chahat, M. Zhadobov, L. Le Coq, and R. Sauleau, "Wearable endfire textile antenna for on-body communications at 60 GHz," *IEEE Antennas Wireless Propag. Lett.*, vol. 11, pp. 799–802, 2012.

[23] F. Liu, Z. Zhang, W. Chen, Z. Feng, and M. F. Iskander, "An endfire beam-switchable antenna array used in vehicular environment," *IEEE Antennas Wireless Propag. Lett.*, vol. 9, pp. 195–198, 2010.
[24] *Ansys HFSS, Version 15*, Ansys, Inc., Canonsburg, PA, USA, 2021.

R. GOPIKA (Graduate Student Member, IEEE) received the master's degree in technology from the Indian Institute of Technology Kharagpur, Kharagpur. She is currently pursuing her research on the topic of design and development of radiative wireless power transfer systems with the Indian Institute of Space Science and Technology, Trivandrum, India. Her research interests include energy harvesting arrays, antenna array systems, and feedback systems for wireless power system efficiency improvement. She received the Young Scientist Award from International Union of Radio Science in 2023 and the AP-S Ph.D. Fellowship Award from IEEE Antennas and Propagation Society in 2022. She has also received the Student Travel Grant Award for AP-S/URSI 2022 and her paper was selected for honourable mention in student paper competition in the same conference. She received the Best Paper Award in the IEEE AP-S track of IEEE Recent Advances in Geoscience and Remote Sensing: Technologies, Standards and Applications, India, 2019.

CHINMOY SAHA (Senior Member, IEEE) received the B.Tech., M.Tech., and Ph.D. degrees in radio physics and electronics from the University of Calcutta, Kolkata, India, in 2002, 2005, and 2012, respectively. He is currently working as a Professor with the Department of Avionics, Indian Institute of Space Science and Technology, Department of Space, Government of India. He has visited several International Universities of repute and having collaborative research with the Royal Military College of Canada, Queens University, Canada. He has more than 170 publications, including 45 journal papers in peer reviewed national and international journals and conference proceedings and authored three books with reputed Cambridge University Press, U.K. and Taylor and Francis, USA. His current research interest includes wireless power transfer and energy harvesting, channel modeling for WB/UWB systems, microwave circuits, engineered materials, metamaterial inspired antennas and circuits, reconfigurable and multifunctional antennas for modern wireless applications, mm-wave THz antennas, and antennas and components for space applications. He has received several prestigious awards which includes Indo-French SRTF Fellowship from embassy of France, National Award "AICTE Visvesvaraya Best Teacher Award 2021" received from Union Education minister, Government of India, "IETE Prof. SN Mitra Memorial Award 2021," "Outstanding Teacher Award" in 2019 from the Department of Avionics, IIST, "National Scholarship from Ministry of Human Resource Development" from Government of India, "Outstanding Contribution Award from the AP-MTT Kolkata chapter, "Best Contribution Award for Notable Services and Significant Contributions towards the Advancements of IEEE and the Engineering Profession" from IEEE Kolkata Section and several best paper awards in various international conferences. He is the Founding Chairman of IEEE MTT-S Kerala chapter. He has served as the Chairman of Antennas and Propagation Chapter of IEEE Kerala Section from 2018 to 2019. He is on the board of reviewers of several international journals of repute, including IEEE TRANSACTION IN MICROWAVE THEORY AND TECHNIQUES, IEEE TRANSACTION IN ANTENNAS AND PROPAGATION, IEEE ANTENNAS AND WIRELESS PROPAGATION LETTERS, *IET Microwaves, Antennas and Propagation*, *Electronic Letters*, and *Scientific Reports* (Nature). He is an Associate Editor of IEEE ACCESS and INTERNATIONAL JOURNAL OF RF AND MICROWAVE COMPUTER AIDED ENGINEERING (Wiley) and a Guest Editor-in-Chief for a special issue in the same journal. He is a member of International Committee of AP-S and MTT-S SIGHT, a member of chapter activity committee of IEEE AP-S, and also a current Region-10 coordinator of IEEE MTT Society. He is a Senior Member of International Union of Radio Science and a Life Member of IETE.

YAHIA M. M. ANTAR (Life Fellow, IEEE) received the B.Sc. degree (Hons.) in electrical engineering from Alexandria University, Alexandria, Egypt, in 1966, and the M.Sc. and Ph.D. degrees in electrical engineering from the University of Manitoba, Winnipeg, MB, Canada, in 1971 and 1975, respectively. In May 1979, he joined the Division of Electrical Engineering, National Research Council of Canada, Ottawa, ON, Canada. In November 1987, he joined the Department of Electrical and Computer Engineering, Royal Military College of Canada, Kingston, ON, Canada, where he has been a Professor since 1990. He has authored or coauthored over 200 journal articles, several books, and chapters in books, over 450 refereed conference papers, holds several patents, has chaired several national and international conferences, and has given plenary talks at many conferences. In 1977, he held a Government of Canada Visiting Fellowship at the Communications Research Center, Ottawa. In 2003, he was awarded the Royal Military College of Canada "Excellence in Research" Prize and the RMCC Class of 1965 Teaching Excellence Award in 2012. In October 2012, he received the Queen's Diamond Jubilee Medal from the Governor-General of Canada in recognition of his contribution to Canada. He was a recipient of the 2014 IEEE Canada RA Fessenden Silver Medal for Ground Breaking Contributions to Electromagnetics and Communications and the 2015 IEEE Canada J. M. Ham Outstanding Engineering Education Award. In May 2015, he received the Royal Military College of Canada Cowan Prize for excellence in research. He was also a recipient of the IEEE-AP-S of the Chen-To-Tai Distinguished Educator Award in 2017. He has supervised and co-supervised over 90 Ph.D. and M.Sc. theses at the Royal Military College and Queen's University, several of which have received the Governor-General of Canada Gold Medal Award, the Outstanding Ph.D. Thesis of the Division of Applied Science, as well as many best paper awards in major international symposia. He served as the Chair for Canadian National Commission, URSI from 1999 to 2008, Commission B from 1993 to 1999, and has a cross-appointment at Queen's University, Kingston. In May 2002, he was awarded the Tier 1 Canada Research Chair in electromagnetic engineering which has been renewed in 2016. He was elected by the URSI to the Board as the Vice President in August 2008 and 2014, and to the IEEE Antennas and Propagation AdCom. In 2019, he was elected as the 2020 President-Elect for IEEE AP-S, and will serve as its President in 2021. He has served as an associate editor for many IEEE and IET journals and an IEEE-APS Distinguished Lecturer. He was appointed as a member of the Canadian Defense Advisory Board of the Canadian Department of National Defense in January 2011. He is a Fellow of the Engineering Institute of Canada and the Electromagnetic Academy. He is also an International Union of Radio Science Fellow.